Journal of Experimental and Theoretical Physics, Vol. 101, No. 3, 2005, pp. 427–436.
Translated from Zhurnal Éksperimental'noĭ i Teoreticheskoĭ Fiziki, Vol. 128, No. 3, 2005, pp. 497–507.

ORDER, DISORDER, AND PHASE TRANSITIONS IN CONDENSED SYSTEMS

Determining the Structural Parameters of Fractal and Nonfractal Objects in Multiple Small-Angle Neutron Scattering Experiments

G. P. Kopitsa[a], S. V. Grigoriev[a], V. V. Runov[a], V. M. Garamus[b], and D. Bellmann[b]

[a] *Petersburg Nuclear Physics Institute, Russian Academy of Sciences, Gatchina, Leningradskaya oblast, 188300 Russia*
[b] *GKSS Research Centre, D-21502 Geesthacht, Germany*
e-mail: kopitsa@mail.pnpi.spb.ru

Received November 10, 2004

Abstract—An experimental procedure employing setups with standard resolution characteristics for multiple small-angle neutron scattering in fractal and nonfractal media is described. Specific features of the proposed method, which are related to a limited resolution of the spectrometer, are considered in the case of large-scale inhomogeneities with the characteristic size exceeding the inverse spatial resolution. A new approach to the extraction of information about the fractal dimension of the system studied is demonstrated, which takes into account the dependence of the attenuation and broadening of the transmitted neutron beam on the sample thickness. © *2005 Pleiades Publishing, Inc.*

1. INTRODUCTION

The method of small-angle neutron scattering (SANS) is widely used for the investigation of nuclear and magnetic inhomogeneities in various materials, including porous media, alloys, etc., which contain a high concentration of contrast inhomogeneities with sizes spread over the scale from tens of ångstöms to several hundred microns. The SANS experiments in such media usually reveal a power dependence of the scattering intensity I on the momentum transfer (scattering vector) q,

$$I(q) \propto q^{-\Delta}, \quad \Delta \le 4,$$

in a certain interval of $q > 1/R$, where R is the characteristic scale of the scattering system. There is a commonly accepted trend to perform SANS measurements in the regime of single scattering (that is, under the condition that $L < l$, where L is the sample thickness and l is the neutron mean free path in the medium) and treat the possible multiple scattering (multiple SANS, MSANS) as a factor complicating the interpretation of data. The value of Δ or its deviation from the Porod asymptotics ($\Delta = 4$) is used to judge on the fractal character (dimension) of the system and on the correlator of scattering inhomogeneities (for more detail, see [1–3]). However, an analysis of the SANS data in this limit hardly allows one to extract information concerning the characteristic scale of the scattering system (of course, except for the possibility of scale evaluation from the uncertainty relation). Information of this kind can be obtained in the case of $q < 1/R$ corresponding to the passage to the Guinier regime [4]. However, both the $q < 1/R$ asymptotics and the Guinier regime are difficult to access for the scattering in strongly dispersive media with high concentrations of inhomogeneities. Moreover the condition $L < l$ frequently cannot be satisfied because of the difficulties of preparing sufficiently thin samples; in such cases, the scattering unavoidably has a multiple character.

This paper considers the possibility of evaluating, in principle, the characteristic scale of a scattering system by measuring both the broadening w of a transmitted neutron beam and the neutron mean free path in the sample using the standard SANS setups in the regime of elastic multiple scattering ($L > l$). The mean free path can be estimated from data on the attenuation of the primary beam as a function of L due to the scattering by angles $\Omega > \Omega_{\min}$, where $\Omega_{\min}$ is determined by the resolution of the instrument. Methods for the estimation of characteristic size using the beam broadening in the neutron scattering experiments has been widely used and extensively developed in both experimental and theoretical aspects, beginning with the work of Weiss [5] (see, e.g., [6–8] and references therein). One aim of this paper is to draw the attention to the relative character of estimates obtained from simultaneous measurements of the beam broadening and the integral cross section of scattering for the angles $\Omega > \Omega_{\min}$. In other words, the resolution of the SANS setup restricts the possibilities of studying the large-scale inhomogeneities both in the case of single scattering and in the multiple scattering regime. Despite this restriction, MSANS is a powerful tool for the investigation of various substances and the determination of structural parameters of fractal and nonfractal objects. However, it should be recognized

that the real task of such investigations is to experimentally evaluate the characteristic scale of inhomogeneities making the main contribution to the scattering measured in the resolution limits of a given instrument, rather than analyzing the spectrum of inhomogeneities that may spread up to sizes that go unrecorded because of the limited resolution. This paper presents an experimental realization of this approach and shows examples of the application of MSANS to determining the structural parameters of systems.

It should be emphasized that multiple scattering substantially differs from the single scattering event. Indeed, in the latter case, the information is obtained using the coherent properties of radiation: the incident and scattered neutron waves are considered as coherent. In contrast, multiple scattering is a diffusion process, and what we measure in experiment is the degree of coherence. In this context, it is interesting to consider MSANS using the concept of coherent or correlation volume of the neutron beam [9].

The correlation volume can be intuitively defined as a region where the coherent properties of neutrons are significant. These properties are described using the correlation function of a collimated beam, which, in turn, is a Fourier image of the instrument resolution function. It should be noted that the correlation length for such a volume in SANS experiments may reach 1000 Å.

When a neutron beam propagates in a medium and exhibits multiple scattering, the correlation length decreases, which reflects the loss of the beam coherence, which leads to broadening of the instrumental linewidth. Naturally, this loss of coherence depends only on the number of scattering events per unit range (scattering length) or, in other words, on the general integral cross section of neutron scattering. The attenuation of the neutron beam is related to decaying amplitude of the neutron wave inside the coherent volume. This amplitude consists of two components, the amplitudes of nonscattered and forward-scattered waves. Obviously, both the correlation length and the amplitude of the neutron wave within this length depend on the properties of a scattering medium.

For this reason, the second but no less important task of this study is to consider the possibility of extracting information about the fractal properties of the scattering medium from data on the broadening and attenuation of a neutron beam in the regime of multiple scattering. One difficulty in obtaining reliable information on the fractal dimension of the medium in the regime of single scattering is related to the need for studying the scattering intensity distribution $I(q)$ in a broad range of q (over more than three orders of magnitude), which is practically impossible for most existing SANS setups. The possibility of obtaining such estimates from data on multiple scattering was demonstrated by Maleyev [3].

The aforementioned problems will be considered based on the results of MSANS, SANS and ultra-small-angle neutron scattering (USANS) experiments described below. The measurements were performed for the model samples of YBCO ceramics, Al_2O_3 powder, limestone ($CaCO_3$) powder, and carbon (C) carbon black in a range of sample thicknesses $L/l < 5$.

The paper is organized as follows. Section 2 briefly summarizes the main stipulations of the MSANS theory developed in [3, 6, 10, 11], which are used below for the interpretation of experimental data. The experimental part is presented in Section 3. The results of experimental data processing are presented and discussed in Section 4, and Section 5 summarizes the main conclusions.

2. THEORY

Let us briefly consider the main stipulations of the theory developed in [3, 6, 10], which are used below for the interpretation of the results of MSANS measurements in various regimes. The aforementioned papers considered the regimes of diffraction [3] for $\alpha \ll 1$ and refraction [10] for $\alpha \gg 1$, where $\alpha = kR(U/E)$ is a change in the neutron wavefunction over an inhomogeneity scale R, $k = 2\pi/\lambda$, is the wavevector of neutrons with the energy E, $U = 2\pi\hbar^2\Delta(bN_0)/m_n$ is the potential energy of the inhomogeneity (optical potential), m_n is the neutron mass, $\Delta(bN_0)$ is the difference of the densities of the scattering lengths for the inhomogeneity and the medium, b is the coherent scattering amplitude, and N_0 is the number of formula units per unit volume (cm^3). The regime of refraction was analyzed in the limit of low concentrations of inhomogeneities in the sample, that is, under the condition that $\delta V/V \ll 1$, where V is the sample volume and δV is the volume fraction accounting for inhomogeneities of the characteristic scale R.

It was shown [3] that the characteristic momentum, which determines the beam broadening as a result of multiple scattering ($L > l$) from a fractal medium in the diffraction regime in the general case, can be written as

$$q_L^{(\Delta)} = \frac{1}{2R}\left(\frac{L}{g_\Delta l}\right)^\mu, \quad \alpha \ll 1, \tag{1}$$

where $\Delta = D_v$ ($D_v < 3$ is the dimension of a volume fractal) or $\Delta = 6 - D_s$ ($2 < D_s < 3$ is the dimension of a surface fractal); $\mu = f(\Delta)$; and $g_\Delta \approx 1$. Accordingly:

$$q_L^{(\Delta)} \propto L^{\mu_{v,s}}, \quad \mu_v = (D_v - 2)^{-1} > 1,$$

$$1/2 < \mu_s = (4 - D_s)^{-1} < 1.$$

In the particular case of $\Delta = 4$ (the Porod asymptotics), we have $\mu = 1/2$ and the scattering intensity $I(q)$ is

described by the diffusion formula:

$$I(q) \propto \exp\left(-\frac{q^2}{2q_L^2}\right), \quad q_L = \frac{1}{2gR}\sqrt{\frac{L}{l}}. \tag{2}$$

Taking into account corrections for the insufficiently rapid decrease in the single scattering cross section with increasing scattering angle [6], the characteristic momentum can be written as

$$q_L = \frac{1}{2R}\sqrt{\frac{L}{l}\ln\frac{L}{l}}, \tag{3}$$

where the mean free path length is given by the formula

$$l = \frac{k^2}{3\pi[\Delta(bN_0)]^2 R}\frac{V}{\delta V}. \tag{4}$$

According to [3], the scattering intensity distribution $I(q)$ in the regime of multiple scattering ($L > l$) is divided into two parts. The asymptotic part (for $q \geqslant q_L^{(\Delta)}$) is similar to the $I(q)$ distribution in the single scattering regime. In the central part (for $q \leq q_L^{(\Delta)}$), the distribution is close to that in the Guinier regime:

$$I(q) = I(0)\left[1 - \frac{q^2 R_g^2(L)}{3}\right]. \tag{5}$$

Here, $R_g(L)$ is the effective gyration radius defined as

$$R_g^2(L) = \frac{3\Gamma(4\mu)}{4\Gamma(2\mu)(q_L^{(\Delta)})^2}, \tag{6}$$

where $\Gamma(x)$ is the gamma function.

The intensity $I(q = 0)$ of forward scattering (i.e., the attenuation) is expressed as [3]

$$I(q=0) = \frac{\mu\kappa^2\Gamma(2\mu)}{2\pi(q_L^{(\Delta)})^2} = \frac{2\mu(\kappa R)^2}{\pi}\left(\frac{g_\Delta l}{L}\right)^{2\mu}\Gamma(2\mu), \tag{7}$$

where $2\mu = 2/(D_v - 2) > 2$ and $1 < 2\mu = 2/(4 - D_s) < 2$ for the volume and surface fractals, respectively, and κ is the neutron wavevector. In both cases, the intensity $I(q = 0)$ decreases with the sample thickness L faster than according to the L^{-1} law (characteristic of the diffusion model used for analysis of MSANS on inhomogeneities with sharp boundaries ($2\mu = 1$)). This behavior of $I(q = 0)$ (as well as of $q_L^{(\Delta)}$) in the case of MSANS in fractal media offers an example of the so-called anomalous diffusion (superdiffusion) [12].

In the regime of refraction [10] in a sample with a small concentration of spherical inhomogeneities and a not very large thickness ($l \ll L \ll L_0 = l\alpha^2\ln\alpha$), the intensity of multiple scattering is also described by a diffusion formula with the characteristic momentum

$$q_1 = \sqrt{\frac{L}{l}\ln\frac{\alpha^2 L}{2l}}\frac{kU}{2E}. \tag{8}$$

For $L \approx L_0$, the scattering intensity deviates from the behavior predicted by the diffusion model, and for $L \gg L_0$ it is described by the formula [10]

$$I(q) = \frac{k^2 q_2}{2\pi(q^2 + q_2^2)^{3/2}}, \quad q_2 = \frac{L}{2g_\Delta lR}. \tag{9}$$

In the asymptotic limit $q \gg q_2$, the intensity of multiple scattering coincides with that of a single scattering and decreases as q^{-3} [10].

To our knowledge, multiple scattering in the refraction regime—neither in the case of a high concentration of inhomogeneities (whereby $\delta V \sim V$ as in multidomain polycrystalline ferromagnets, granulated and ceramic materials, etc.), nor in fractal media—has not been considered in the literature.

3. EXPERIMENT

In our MSANS experiments, the attenuation $I(q = 0)/I_0$, the broadening w of the neutron beam, and the scattering intensity $I_s(q)$ (for 5×10^{-3} Å$^{-1} < q < 3.5 \times 10^{-2}$ Å^{-1}) were studied as functions of the sample thickness L for YBCO ceramics, Al_2O_3 powder, $CaCO_3$ powder, and carbon black. The sample parameters important from the standpoint of MSANS were as follows:

(i) $YBa_2Cu_3O_{7+\delta}$ (YBCO) ceramics: $bN_0 = 4.75 \times 10^{10}$ cm^{-2}; density, $\rho \approx 4.9$ g cm^{-3}; range of sample thicknesses, L is from 0.9 to 20 mm; $\delta L/L \leq 1.5\%$.

(ii) Al_2O_3 powder: $bN_0 = 5.38 \times 10^{10}$ cm^{-2}; average grain size, 18–20 μm; L is from 2 to 16 mm; $\delta L/L \leq 2.5\%$.

(iii) Limestone ($CaCO_3$) powder: $bN_0 = 5.11 \times 10^{10}$ cm^{-2}; $\rho \approx 2.93$ g cm^{-3}; L is from 0.1 to 8.9 mm; $\delta L/L \leq 1.5\%$.

(iv) Carbon black: $bN_0 = 6.5 \times 10^{10}$ cm^{-2}; L is from 0.2 to 9 mm; $\delta L/L \leq 1.5\%$.

The MSANS measurements were performed using the small-angle polarized neutron scattering facility Vector-20 (WWR-M reactor, Petersburg Nuclear Physics Institute, Russian Academy of Sciences, Gatchina), which operated in slit geometry with twenty ^{3}He detectors in the horizontal plane [6]. The scattering intensity could be scanned in a range of q up to 5×10^{-1} Å^{-1} by rotating the detector system. In this experiment, the polarization technique was used for monochromatization of the neutron beam monochromatic. The measurements were performed at a neutron wavelength of $\lambda = 8$ Å with $\Delta\lambda/\lambda = 9\%$, which excluded the Bragg scattering. The vertical and horizontal resolution calculated

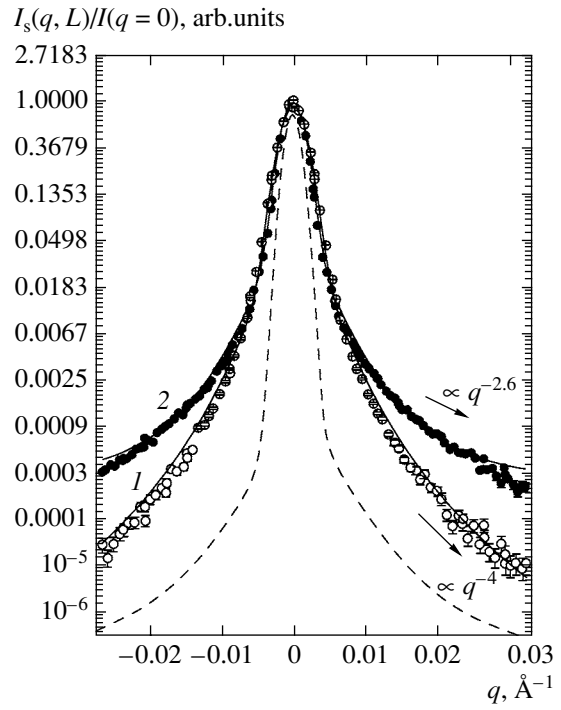

Fig. 1. The neutron beam shape measured in a regime of single scattering ($L < l$): (open circles) $CaCO_3$, $L = 0.67$ mm; (black circles) carbon black, $L = 0.83$ mm. Solid curves *1* and *2* show the results of calculations using formula (10); dashed curve represents the beam shape in the absence of a sample.

with allowance for the slit geometry [14] of the experimental setup was $\delta q_v = 3 \times 10^{-3}$ Å^{-1} and $\delta q_h = 8 \times 10^{-4}$ Å^{-1}, respectively.

In order to obtain independent data on the fractal dimension of carbon black and verify the MSANS results, we additionally studied this sample using the traditional SANS and USANS techniques in a broad range of momentum transfer ($1.5 \times 10^{-6} < q < 1.5 \times 10^{-1}$ Å^{-1}). The SANS measurements were performed using the SANS-1 facility (FRG1 reactor GKSS Research Centre, Geesthacht, Germany) [15], which operated in a geometry close to point geometry and was equipped with a two-dimensional (2D) position-sensitive ^{3}He detector. The working neutron wavelength was $\lambda = 8.1$ Å with $\Delta\lambda/\lambda = 10\%$. The experiments were performed for four distances between the sample and detector $R_{sd} = 0.7$, 1.8, 4.5, and 9.7 m, which allowed the momentum transfer to be varied within $3 \times 10^{-3} < q < 1.5 \times 10^{-1}$ Å^{-1}). The instrument resolution was approximated by the Gauss function and calculated separately for each R_{sd} value as described in [16].

The carbon black sample was placed in a 1-mm-thick quartz cell. The initial spectra measured in each q interval were corrected using standard procedures with allowance for scattering from the setup parts and the cell and for the room background [17]. The obtained 2D spectra were averaged with respect to azimuth and normalized to the cross section of noncoherent neutron scattering in a 1-mm-thick layer of water [17]. For $R_{sd} >$ 1.8 m, the spectra were normalized to the cross section determined for $R_{sd} = 1.8$ m with additional allowance for the attenuation factor [17].

The USANS measurements were performed using a DCD double crystal diffractometer (at the same FRG1 reactor of the GKSS Research Center) at a working neutron wavelength of $\lambda = 4.43$ Å with $\Delta\lambda/\lambda = 1 \times 10^{-5}$ [18]. This instrument was equipped with a double monochromator unit based on perfect silicon crystals cut along the (1, 1, 1) plane. The first crystal was used to form the neutron beam and the second crystal performed the monochromator function. The angular distribution of neutrons in the beam past the sample (situated behind the double monochromator) was measured by rotating an analyzer crystal (identical to the monochromator crystal) at a minimum angular step of 2×10^{-7} deg. The FWHM of the instrument line was $w_0 = 2.6 \times 10^{-5}$ Å^{-1}. The momentum transfer was varied within $1.5 \times 10^{-6} < q < 5 \times 10^{-3}$ Å^{-1}.

Figures 1–3 show the pattern of typical changes in the shape of the neutron beam, $I_s(q)/I(0)$, and in the attenuation I/I_0 (where $I_0 = I(L = 0)$), measured by the central detector as $I(q = 0)$ as a function of the sample thickness.

The experimental beam attenuation profiles (Fig. 3) are normalized to the integral attenuation cased by neutron absorption in the samples.

4. RESULTS AND DISCUSSION

4.1 MSANS

4.1.1. Beam shape. It was found that the shape of the neutron beam upon scattering can be represented as a sum of two components: Gaussian, describing the beam width upon scattering, and Lorentzian of nth power ($n = f(\Delta)$), describing the dependence of the scattering intensity $I_s(q, L)$ on q at large momenta:

$$I(q) = A\exp\left[-\frac{(q - q_{01})^2}{2s^2}\right] + B\frac{sr^{2n}}{[(q - q_{02})^2 + sr^2]^n} + C, \quad (10)$$

where A, B, C, s, and n are free parameters and q_{01} and q_{02} are the centering parameters. The quantity $sr^2 = \delta q_v^2 + s_1^2$ is a sum of dispersions determining the momentum uncertainty in the beam (s_1 is the s value determined by fitting the experimental data to formula (10) for $sr^2 = \delta q_v^2$). The uncertainty δq_h related to the horizontal resolution (which is almost ten times as small as the verti-

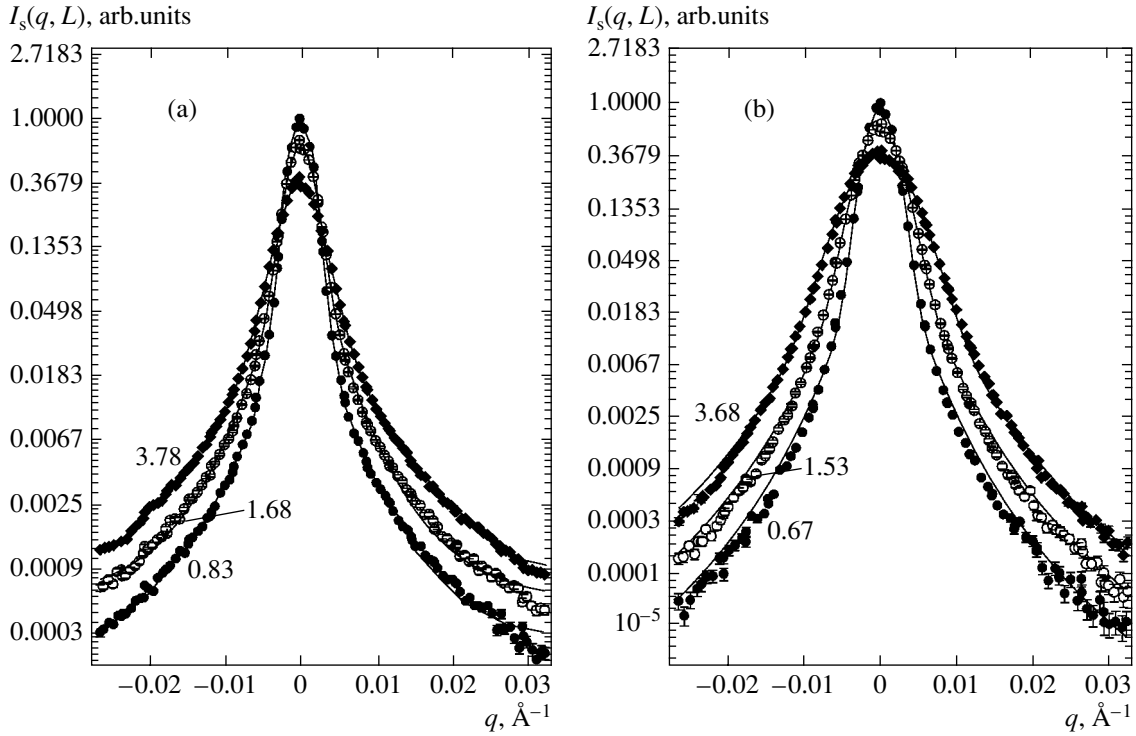

Fig. 2. Variation of the neutron beam shape for (a) carbon black and (b) $CaCO_3$ samples of different thickness L (indicated in millimeters at the curves). Points present the experimental data; solid curves show the results of calculations using formula (10).

cal resolution) is reflected predominantly by the s value, since

$$s^2 = \Delta w^2(L) + s_0^2, \tag{11}$$

where $\Delta w(L)$ is the beam broadening in a sample of thickness L and s_0 is the beam dispersion in the absence of the sample. In the course of fitting by least squares to formula (10), it was established that the dispersion s varies rather slightly and falls almost within the experimental error limits, irrespective of the fact whether this value is taken into account or not in the sr product (i.e., $s \approx s_1$). However, only allowance for the s value in the sr product provides a satisfactory description of scattering in the region of "tails". Substitution of a preset value of s_1 instead of the free parameter s into the sr product significantly simplifies the fitting procedure. Depending on the sample thickness, the sr product values fall within $sr = (5–6.5) \times 10^{-3}$ Å^{-1} (YBCO), $(5–8) \times 10^{-3}$ Å^{-1} ($CaCO_3$), $(5–8.5) \times 10^{-3}$ Å^{-1} (Al_2O_3), and $(5–7) \times 10^{-3}$ Å^{-1} (carbon black). The fitting by least squares gives the following values of exponent in formula (10): $n = 2$ ($CaCO_3$, Al_2O_3, YBCO) and $n = 1.3$ (carbon black). The dependences calculated using formula (10) with the parameters found through fitting by least squares are depicted by solid curves in Figs. 1 and 2.

4.1.2. Scattering intensity $I_s(q)$. Figure 4 shows the plots of $I_s(q)$ versus momentum q at $q > sr$ for $CaCO_3$ and carbon black (analogous curves were also obtained for Al_2O_3 and YBCO). It was found that these dependences could be satisfactorily described using the formula

$$I_s(q) = A_1/q^{\Delta}, \tag{12}$$

where $\Delta = 4 \pm 0.1$ (for $CaCO_3$, Al_2O_3, YBCO) or 2.6 ± 0.1 (for carbon black) and the parameter A_1 is virtually a linear function of L. The scattering data were processed by least squares (with corrections for the slit geometry) and analyzed in the range of momentum transfer 0.007 Å$^{-1} \le q \le 0.03$ Å^{-1}. A correction for the slit geometry is essential for $q < 10^{-2}$ Å^{-1}, where the experimental data (representing a convolution of the scattering intensity $I_s(q) \propto q^{-\Delta}$ with the instrument resolution function) deviate from the $q^{-\Delta}$ law (these deviations are not distinguished in Fig. 4). The power dependence of the scattering intensity on the momentum $I_s(q, L) \propto q^{-2.6}$, which is observed for carbon black, is similar to that for scattering on a volume fractal with the dimension $D_v = 2.6 \pm 0.1$.

4.1.3. Beam attenuation. For small sample thicknesses ($L < l$), the attenuation of the central beam as a function of L for all samples (Fig. 3) could be satisfactorily described using the formula

$$\frac{I(q = 0)}{I_0} = \exp\left(-\frac{L}{l_{\exp}}\right), \tag{13}$$

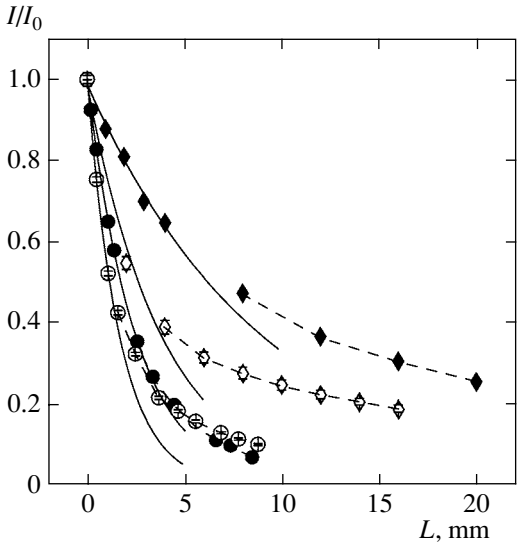

Fig. 3. Attenuation of the beam intensity measured using the central detector for neutrons scattered with a momentum transfer $q > q_{min}$ (q_{min} is determined by the instrument resolution) as a function of the sample thickness L: (●) carbon black; (○) $CACO_3$; (♦) YBCO; (◊) Al_2O_3. Solid curves show the results of fitting to the $\exp(-L/l_{exp})$ law; dashed curves show the results of calculations using formula (14).

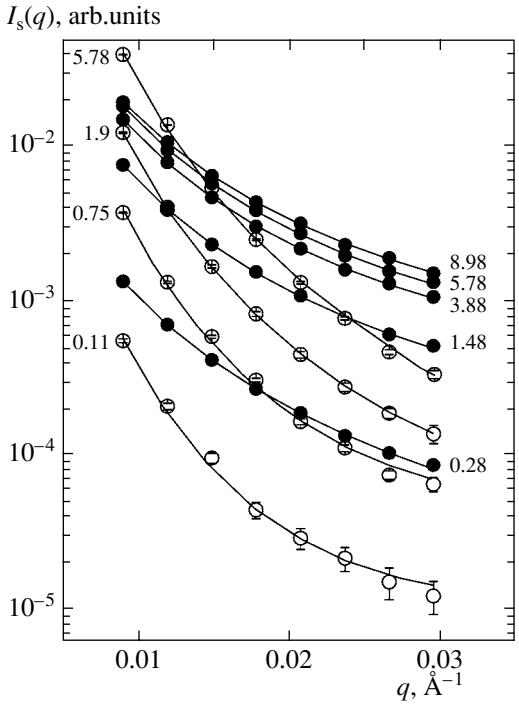

Fig. 4. Plots of the neutron scattering intensity $I_s(q)$ versus momentum transfer q ($q > sr$) for (●) $CaCO_3$ and (○) carbon black samples of various thicknesses L (indicated in millimeters at the curves). Solid and dashed curves show the results of fitting to the $I_s \propto q^{-\Delta}$ law. For all sample thicknesses, $\Delta = 4 \pm 0.6$ ($CaCO_3$) and 2.6 ± 0.01 (carbon black).

which was used for determining the neutron mean free path l_{exp}. The results of l_{exp} determination by this method are presented in Table 1. The calculated curves of I/I_0 versus L for the parameters determined by least squares are depicted by solid lines in Fig. 3.

As can be seen from Fig. 3, an increase in the sample thickness is accompanied by deviation of the experimental data from the exponential dependence, which is related to the multiple scattering. It was found that experimental data on the beam attenuation with increasing sample thickness for nonfractal objects are well described with allowance for multiple scattering in terms of expression (2) within the limits of the vertical and horizontal resolution of the central detector. The 2D convolution of the diffusion formula (2) at $q = 0$ with the instrument resolution functions in the two directions described by Gaussians with dispersions δq_h and δq_v, which was used for processing the data on the beam attenuation for $L > 0.5 l_{exp}$, is as follows:

$$\frac{I}{I_0} = \frac{2D\delta q_x \delta q_y}{\{[(2\delta q_x)^2 + FL][(2\delta q_y)^2 + FL]\}^{\mu}}, \qquad (14)$$

where D and F are free parameters and $\mu = 1/2$.

Table 1. The main parameters of samples determined from an analysis of the MSANS data (see the text for explanations)

Sample	l_{exp}, mm	Δ	μ	D	R, Å
Nonfractal					
Al_2O_3	3.9 ± 0.6	4 ± 0.6	0.5	3	203 ± 11
YBCO	9.4 ± 0.3	4 ± 0.6	0.5	3	171 ± 16
$CaCO_3$	1.7 ± 0.1	4 ± 0.1	0.5	3	216 ± 6
Fractal					
C (carbon black)	2.5 ± 0.1	2.6 ± 0.1	0.8 ± 0.1	$D_v = 2.6 \pm 0.1$*	
				$D_s = 2.75 \pm 0.15$**	351 ± 12

*From large-q asymptotics.

**From data on the neutron beam broadening and attenuation.

The results of least squares fitting to formula (14) for $CaCO_3$, Al_2O_3, and YBCO are depicted by dashed lines in Fig. 3. Expression (14) shows that, in the limit of $\delta q_x, \delta q_y \longrightarrow 0$, the attenuation asymptotically tends to $I/I_0 \propto 1/L$ in agreement with the theory [3]. The quantity F in formula (14) was treated as a free parameter, but, if the deviation of the beam attenuation from exponent is completely described by the diffusion formula (2) within the aperture of the central detector, we must have $FL = 2q_L^2$. Calculations showed that this relation is valid to within 3%, provided that the beam attenuation is measured in an optimized geometry ($\delta q_v = 1.8 \times 10^{-3}$ Å^{-1}), where q_L are taken from an analysis of data on the beam broadening (Fig. 5).

We have also used formula (14) in the analysis of data on the beam attenuation at $L > 0.5 l_{exp}$ for carbon black, but the exponent μ was treated as a free parameter. Then, the fitting by least squares gave $\mu = 0.8 \pm 0.1$. In the limit of $\delta q_x, \delta q_y \longrightarrow 0$, this yields the asymptotic behavior $I/I_0 \propto 1/L^{2\mu}$ with $2\mu = 1.6$. According to the theory [3], this behavior corresponds to the neutron beam attenuation upon multiple scattering on the surface fractal with the dimension $D_s = 4 - 1/\mu = 2.75$.

4.1.4. Beam broadening. Figure 5 presents our experimental data on the beam broadening as a function of the sample thickness, which was determined from relation (11) as

$$\Delta w^2 = s^2 - s_0^2. \quad (15)$$

As will be shown below, the characteristic scale of inhomogeneities determined in our experiments is on the order of several hundred ångströms. For this reason, the experimental data can be described in the diffraction approximation. Estimates show that the characteristic size R_0 (corresponding to $\alpha \approx 1$) at which the refraction regime also becomes significant is $R_0 \approx 2 \times 10^{-3}$ mm. The corresponding characteristic momentum according to Eq. (8) is $q_1 < 2 \times 10^{-4}$ Å^{-1}. Thus, the refraction scattering component corresponds to the range of momenta below the limiting resolution of the instrument and, hence, this component can be ignored in comparison to diffraction in the analysis of scattering. Analogous estimates were previously reported in [11] for SANS in YBCO ceramics.

As can be seen from Fig. 5, the beam broadening defined as $\Delta w = q_L$ (see Eqs. (1)–(3)) is satisfactorily described by the formula

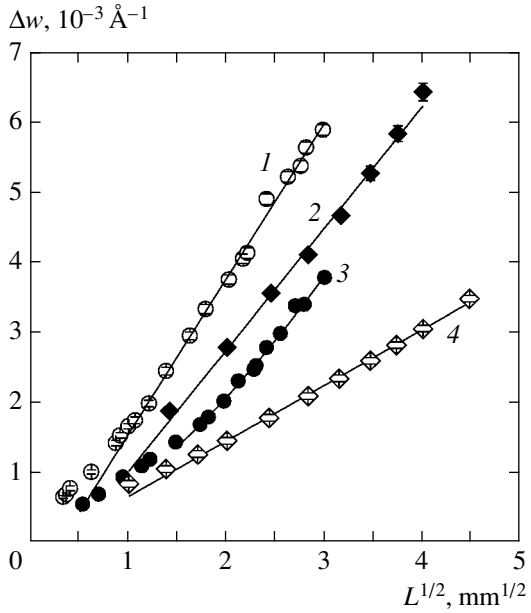

Fig. 5. Plots of the beam broadening $\Delta w = \sqrt{w^2 - w_0^2}$ versus sample thickness L for (*1*) $CACO_3$; (*2*) YBCO; (*3*) carbon black, and (*4*) Al_2O_3. Points present the experimental data; solid curves show the results of calculations using the formula $\Delta w = a + bL^{\mu}$.

$$\Delta w = a + bL^{\mu} \quad (16)$$

with a nonzero "cutoff" on the abscissa axis for $L \longrightarrow 0$. This relation was considered in much detail in [6–8]. An analysis of the data on $\Delta w(L)$ gave the following values of the exponent: $\mu = 0.5$ (for $CaCO_3$, Al_2O_3, YBCO) or ~0.8 (for carbon black), which is fully consistent with the values obtained above from the analysis of the central beam attenuation I/I_0 as a function of the sample thickness L.

Within the framework of the diffraction approximation, the characteristic size R of inhomogeneities making the main contribution to the scattering detected within the limits of resolution of a given instrument can be determined using formula (1) with the aforementioned parameters l_{exp} and q_L. These estimates of R in all samples under consideration for $L \geq l_{exp}$ are presented in Table 1 and plotted in Fig. 6, where solid and dashed curves show the data calculated using formula (16).

The scattering from inhomogeneities on this scale must lead to deviations from power dependences of the scattering intensity (Fig. 4) for $sr < q \leq 1/2R$. However,

Table 2. Fractal dimensions determined by analysis of the SANS data for carbon black

Interval of q, Å^{-1}	0.048–0.15	0.013–0.064	0.007–0.022	0.003–0.009
Fractal dimension D	2.54 ± 0.1	2.75 ± 0.05	2.56 ± 0.08	2.62 ± 0.02

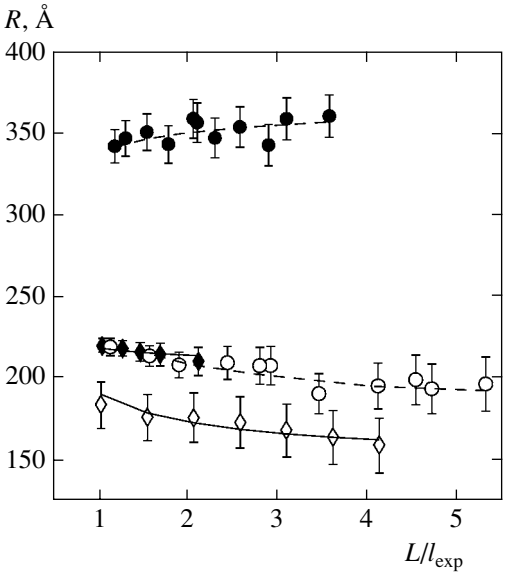

Fig. 6. Plots of the characteristic scale R of the scattering system versus L/l for (●) carbon black, (○) $CACO_3$; (♦) YBCO; and (◊) Al_2O_3. Points present the results of calculations using formula (5); solid and dashed curves show the results of fitting using formula (16).

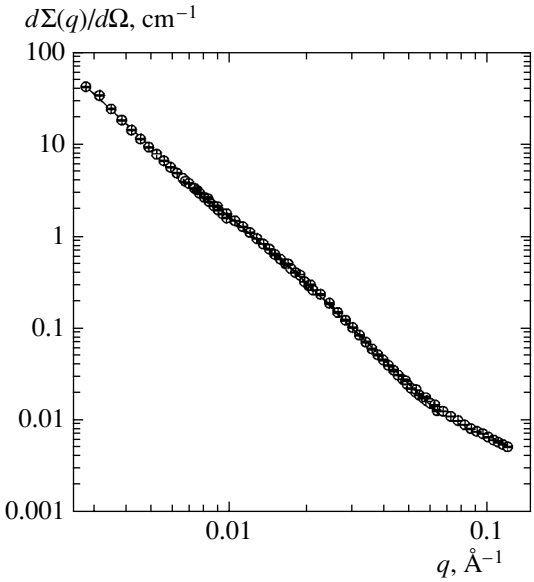

Fig. 7. A plot of the differential cross section of neutron scattering $d\Sigma(q)/d\Omega$ versus momentum transfer for a sample of carbon black with $L = 1.5$ mm. Points present the results of SANS measurements; solid curve shows the results of calculations using expression (17).

this condition was not met in our experiments, where the minimum sr value was $sr_{min} \approx 3 \times 10^{-3}$ Å^{-1}. In order to observe deviations from the power dependence of the scattering intensity at low q, the experiments have to be performed using thin samples and an experimental setup with sufficient resolution for a momentum transfer of $q < 10^{-3}$ Å^{-1}.

4.2. SANS and USANS

As can be seen from the MSANS data in Table 1, which were obtained using measurements of the neutron beam broadening and attenuation as dependent on the sample thickness L ($q \le q_L$), carbon black is a surface fractal with $D_s = 2.75 \pm 0.15$. At the same time, the exponent Δ determined from an analysis of the scattering intensity I_s as a function of the momentum q in the asymptotic limit for $q \gg q_L > 7 \times 10^{-3}$ Å^{-1} is 2.6 ± 0.1, which corresponds to the scattering on a volume fractal with $D_v = 2.6 \pm 0.1$. These results can be explained by assuming that (i) the samples of carbon black under study contain two (surface and volume) fractals and (ii) the main contributions of these fractals to the scattering intensity $I_s(q)$ are observed in different ranges of q. This implies that $I_s(q)$ plotted on the logarithmic scale must exhibit a bending point, which corresponds to the passage from one type of scattering to another. In order to check for this assumption, it was necessary to obtain independent estimates of the fractal dimension of carbon black. Such estimates can be obtained by measuring the neutron scattering intensity distribution $I_s(q)$ using the SANS and USANS techniques in a single scattering regime in the most broad range of the momentum transfer q.

Figure 7 shows a plot of the differential cross section of neutron scattering $d\Sigma(q)/d\Omega$ measured for a sample of carbon black with $L = 1.5$ mm using the SANS-1 setup in the momentum range 0.003 Å$^{-1} \le q \le 0.15$ Å^{-1}. The data were analyzed in terms of the formula

$$\frac{d\Sigma}{d\Omega}(q) = \frac{A_2^2}{q^D} + I_{inc}, \qquad (17)$$

where A_2 is a free parameter and I_{inc} is a constant quantity, which is independent of q and related to the scattering from inhomogeneities on the order of the wavelength λ (in this case, from one to several tens of ångströms). The final results were obtained by calculating a convolution of expression (17) with the instrument resolution function. The experimental curves of the differential cross section $d\Sigma(q)/d\Omega$ were processed by least squares for each of the four intervals of variation of the q value. The results of this analysis are summarized in Table 2.

As can be seen from the data in Table 2, the fractal dimensions fall within 2.54–2.75 depending on the interval of q values used for the analysis. At the same time, the fractal dimension ($D \approx 2.65$) obtained by averaging over all the q intervals under consideration is close to the estimate $D_v = 2.6 \pm 0.1$ obtained for the same sample of carbon black in our MSANS experiments.

Figure 8 shows the results of USANS measurements for the carbon black samples with $L = 0.2$ and 1.5 mm

measured using a double crystal diffractometer [18]. The attenuation of the neutron beam transmitted through the sample was very large: $1 - I(q = 0)/I_0 \approx 0.84$ and 0.97 for 0.2- and 1.5-mm-thick samples, respectively. This implies that the experimental data should be interpreted in terms of the MSANS theory [3]. In the standard analysis of USANS spectra for $L > l$, parameters characterizing the scattering system are usually determined from the $\Delta w(L)$ function [7, 8]. In the case under consideration, we are interested in determining the asymptotic behavior of $I(q)$ at large q. As was pointed out above (and demonstrated previously [3, 6, 9, 18]), the character of this behavior is similar to that in the case of single scattering.

We have analyzed the scattering intensity $I(q)$ at large q using a procedure described in [19]. According to this, the experimental data are approximated using a function of the type

$$I(q) = \frac{A_3}{q^2} + \frac{A_4}{q^\delta}, \qquad (18)$$

where the first term describes the scattering intensity variation on the wings of the instrument function and the second term reflects the asymptotic behavior of the scattering at large q in the sample studied. The values of the exponent δ determined by least squares fitting to formula (18) for $L = 0.2$ and 1.5 mm were $\delta = 2.35 \pm 0.03$ and 2.8 ± 0.03, respectively. According to [19], an increase in δ with the sample thickness is related to the pre-asymptotic terms of the expansion of $I(q)$ at large q. The $I(q)$ values calculated using formula (18) with the parameters determined by least squares are depicted by solid curves in Fig. 8.

For the correct comparison of USANS data to the results obtained in the conventional SANS experiments, it is necessary to take into account that the exponent in the dependence of the scattering intensity on the momentum transfer measured using the double-crystal technique is increased by unity [19]. Therefore, the asymptotic behavior of the scattering intensity $I(q)$ for carbon black in the interval 3×10^{-4} Å$^{-1} \le q \le 3 \times 10^{-3}$ Å^{-1} is satisfactorily described by the relation $I(q) \propto q^{-\Delta}$, where $\Delta = \delta + 1 = 3.35$–$3.38$, which is equivalent to the scattering on a surface fractal with the dimension $D_s = 6 - \Delta = 2.62$–2.65. This value is very close to the estimate ($D_s = 2.75 \pm 0.15$) obtained in our MSANS experiments.

Thus, we have measured the small-angle neutron scattering intensity $I_s(q)$ for carbon black in the range of momentum transfer 0.0003 Å$^{-1} \le q \le 0.15$ Å^{-1} using the SANS and USANS techniques. The obtained data unambiguously indicate that there are two intervals of q in which the scattering intensity $I_s(q)$ obeys the law $I_s(q) \propto q^{-\Delta}$ with different values of the exponent Δ. In the interval of $q \le q_c$ (where $q_c \approx 0.003$ Å^{-1} is the point of bending on the $I_s(q)$ curve), the exponent is close to 3.35, whereas at $q \ge q_c$, we have $\Delta \approx 2.65$. This asymptotic behavior of $I_s(q)$ shows the presence of two correlators, which characterize the system under consideration and predominate in the corresponding interval of q. The first correlator corresponds to a surface fractal with the dimension $D_s = 2.65$, while the second correlator corresponds to a volume fractal with the same dimension $D_v \approx 2.65$.

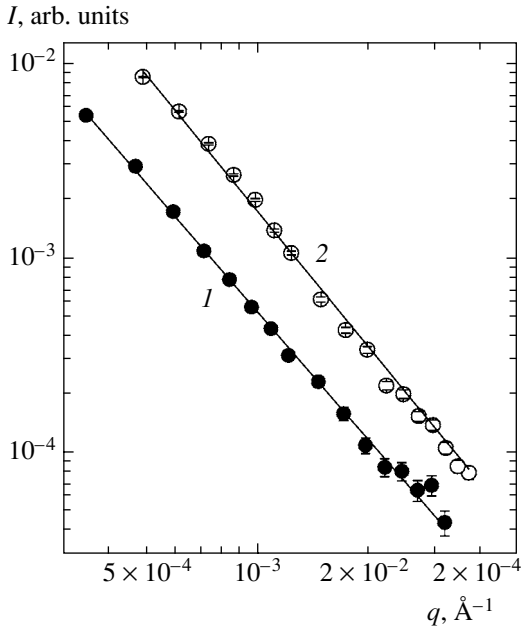

Fig. 8. Plots of the neutron scattering intensity versus momentum transfer for carbon black samples with L = 0.2 (*1*) and 1.5 mm (*2*). Points present the results of USANS measurements; solid curves show the results of calculations using expression (18) for $q \gg q_L$.

5. CONCLUSIONS

(i) We have experimentally demonstrated the possibility of using MSANS method [3, 6, 10] for evaluating the structural parameters (the characteristic scale R and the mean free path l) of a scattering system using the standard instruments where these values cannot be determined in the standard SANS regime.

(ii) A new method has been proposed for estimating the fractal system dimension using data on the attenuation and broadening of the transmitted neutron beam in the MSANS regime.

(iii) A comparison of the MSANS data to the values obtained by the classical SANS and USANS methods in the regime of single scattering showed a good coincidence of the results. In particular, a volume fractal with the dimension $D_v = 2.6 \pm 0.15$ in the asymptotic limit of large q and a surface fractal for carbon black with the dimension $D_v = 2.7 \pm 0.15$ for $q \le q_L$ were observed both in our MSANS experiments and in the SANS and USANS measurements.

ACKNOWLEDGMENTS

The authors are grateful to A.I. Okorokov for his constant attention and support; to S.V. Maleyev, B.P. Toperverg and D. N. Aristov for fruitful discussions and help in interpreting the results, to M.K. Runova for assistance in data processing; to S.A. Klimko for his help in experiments; and to A.I. Sibilev for his help in sample preparation.

This study was supported in part by the Russian Foundation for Basic Research (project no. 04-02-16342), the Federal Program "Investigations of the Basic Properties of Highly Correlated Systems by Neutron Scattering in Constant-Flux Reactors" (project no. 40.012.1.1.1149), and the Presidential Program of Support for Leading Scientific Schools in Russia (project no. NSh-1671-2003.2).

REFERENCES

1. J. K. Kjems, T. Freltoft, D. Richter, and S. K. Sinha, Physica B (Amsterdam) **136**, 285 (1986).
2. S. K. Sinha, Physica D (Amsterdam) **38**, 310 (1989).
3. S. V. Maleyev, Phys. Rev. B **52**, 13163 (1995).
4. A. Guinier and G. Fournet, *Small-angle Scattering of X-rays* (Wiley, New York, 1955).
5. R. J. Weiss, Phys. Rev. **83**, 379 (1951).
6. S. V. Maleev and B. P. Toperverg, Zh. Éksp. Teor. Fiz. **78**, 315 (1980) [Sov. Phys. JETP **51**, 158 (1980)].
7. S. Sh. Shil'shteĭn, V. A. Somenkov, M. Kalanov, and N. O. Elyutin, Fiz. Tverd. Tela (Leningrad) **18**, 3231 (1976) [Sov. Phys. Solid State **18**, 1886 (1976)].
8. Yu. G. Abov, Yu. I. Smirnov, D. S. Denisov, *et al.*, Fiz. Tverd. Tela (St. Petersburg) **34**, 1408 (1992) [Sov. Phys. Solid State **34**, 748 (1992)].
9. R. Gahler, J. Felber, F. Mezei, and R. Golub, Phys. Rev. A **58**, 280 (1998).
10. S. V. Maleyev, R. V. Pomoptsev, and Yu. N. Skryabin, Phys. Rev. B **50**, 7133 (1994).
11. A. I. Okorokov, V. V. Runov, A. D. Tret'yakov, *et al.*, Zh. Éksp. Teor. Fiz. **100**, 257 (1991) [Sov. Phys. JETP **73**, 143 (1991)].
12. J.-P. Bouchaud and A. Georges, Phys. Rep. **195**, 127 (1990).
13. S. V. Grigoriev, V. V. Runov, A. I. Okorokov, *et al.*, Nucl. Instrum. Methods Phys. Res. A **389**, 441 (1997); Preprint No. 2028, PIYaF RAN (Inst. of Nuclear Physics, Russian Academy of Sciences, Gatchina, 1995).
14. W. Schmatz, T. Springer, J. Schelten, and K. Ibel, J. Appl. Crystallogr. **7**, 96 (1974).
15. H. B. Shuhrmann, N. Burkhardt, G. Dietrich, *et al.*, Nucl. Instrum. Methods Phys. Res. A **356**, 133 (1995).
16. J. S. Pedersen, D. Posselt, and K. Mortensen, J. Appl. Crystallogr. **23**, 321 (1990).
17. G. D. Wignall and F. S. Bates, J. Appl. Crystallogr. **20**, 28 (1986).
18. D. Bellmann, M. Klatt, R. Kampmann, and R. Wagner, Physica B (Amsterdam) **241–243**, 71 (1998).
19. Yu. G. Abov, D. S. Denisov, F. S. Dzheparov, *et al.*, Zh. Éksp. Teor. Fiz. **114**, 2194 (1998) [JETP **87**, 1195 (1998)].

Translated by P. Pozdeev